Neutron scattering and specific heat study of AlGe and AlSi alloys quenched under high pressure

1993 J. Phys.: Condens. Matter 5 4737

(http://iopscience.iop.org/0953-8984/5/27/018)

J. Phys.: Condens. Matter 5 (1993) 4737–4748. Printed in the UK

Neutron scattering and specific heat study of AlGe and AlSi alloys quenched under high pressure

A I Kolesnikov†, O I Barkalov†, I T Belash†, E G Ponyatovsky†, J C Lasjaunias‡, U Buchenau§, H R Schober§ and B Frick¶

† Institute of Solid State Physics, Russian Academy of Sciences, 142432 Chernogolovka, Russia

‡ Centre de Recherches sur les Tres Basses Temperatures, BP 166X, F-38042 Grenoble Cedex, France

§ Institut für Festkörperforschung, KFA Jülich, Postfach 1913, D-5170 Jülich, Federal Republic of Germany

¶ Institut Laue–Langevin, BP 156 X, F-38042 Grénoble Cédex, France

Received 18 February 1993

Abstract. Neutron scattering and specific heat measurements on pressure-quenched AlGe and AlSi alloys are reported. The neutron results corroborate earlier findings of a pronounced softening of the transverse zone boundary modes in these polycrystalline non-equilibrium alloys, reminiscent of a similar softening observed in metallic glasses. At lower frequencies, however, no pronounced glassy anomaly is found. The additional excitations seen around 9 meV in AlGe can be explained in terms of resonant modes of the heavier Ge atoms. At still lower frequencies, neutrons see only sound waves. The more sensitive specific heat technique shows the corresponding lattice T^3 term and an electronic contribution which follows the classical BCS behaviour at the transition to superconductivity. Below 0.5 K, there remains a linear term about a factor of ten smaller than in typical glasses.

1. Introduction

The solubility of Ge and Si in Al was recently shown to increase under high pressure to 18 and 20%, respectively [1]. The samples can be quenched under pressure to liquid nitrogen temperature [2], where they remain stable even after removal of the pressure. The samples show a strong increase of the superconducting transition temperature T_c with increasing Si or Ge content; Al with 18% Ge has a T_c of 7.2 K and Al with 20% Si even has 11.0 K, as compared to 1.2 K for pure Al. The thermal stability of the quenched samples allows us to study the interesting physical properties of these alloys.

Chevrier and co-workers [3] reported some glass-like anomalies of $Al_{0.94}Si_{0.06}$, a non-equilibrium substitutional alloy obtained by quenching under high pressure from 1000 K to room temperature. They observed in inelastic neutron scattering experiments a large softening of the transverse acoustic modes, similar to that found in amorphous metals. Another glass-like feature [4] is a linear term in the specific heat below 0.5 K (in the superconducting regime). Measurements of the thermal conductivity and elastic properties [5], however, do not show the behaviour of amorphous metals.

In the related systems $Al_{0.96}Ge_{0.04}$ and $Al_{0.87}Ge_{0.13}$ we found an even stronger enhancement of the vibrational density of states below the transverse zone boundary modes [6]. In contrast to the findings in the AlSi system, the additional excitations do

0953-8984/93/274737+12$07.50

not look like a low-frequency tail of the transverse acoustic modes, but rather like resonant heavy-defect modes around 10 meV, similar to those observed in the system AlAg [7].

In the present work we extend these investigations of AlGe [6] and AlSi [3] alloys to lower-frequency neutron data and higher Si concentrations, using our technique of quenching to liquid nitrogen under high pressure. The paper concentrates on the low-frequency region, where one finds in glasses a mixture of sound waves and additional modes with strongly anharmonic temperature dependence [8, 9]. For the AlGe alloy, we report new low-temperature specific heat measurements between 80 mK and 7 K.

2. Sample preparation

The systems AlGe and AlSi have a simple eutectic phase diagram. The solubility limit of Ge and Si in Al at the eutectic temperature and ambient pressure is $c = 2.6$ and 1.6 at.% [10], respectively. When pressure is applied, the solubility grows. At $P = 7$ GPa and $T = 570$ K one can obtain a substitutional FCC solid solution with 18 at.% of both Ge and Si. The superconducting critical temperature of these alloys increases approximately linearly with the Ge and Si concentration up to $T_c = 7.2$ K and 11.0 K [11] at a concentration of 18 at.% of Ge and Si, respectively (for pure Al, $T_c = 1.2$ K).

The $Al_{0.88}Ge_{0.12}$, $Al_{0.88}Si_{0.12}$ and $Al_{0.92}Si_{0.08}$ mixtures were made molten in graphite crucibles placed in evacuated quartz tubes. Ge and Si of semiconductor quality and 99.99% pure Al were used. To prevent grain growth the ingots were remolten in a vacuum inductance furnace and then quenched in a water cooled copper mould.

The solid solutions were homogenized for 2.5 h at $T = 620$ K and at 6.5 GPa. The high-pressure chamber was then rapidly cooled to liquid nitrogen temperature and the pressure was released. The single-phase state was confirmed by x-ray analysis below $T = 100$ K. All the devices in use allowed us to mount the samples at liquid nitrogen temperature.

The content of Ge and Si in the metastable solid solution was checked by measuring the lattice parameters and the critical superconducting temperatures. The data agreed well with those obtained earlier [1].

3. Neutron experiments

3.1. Experimental

The neutron measurements were done on the time-of-flight spectrometer IN6 placed at the cold-neutron guide of the High Flux Reactor of the Institut Laue–Langevin at Grenoble. The wavelength of the incoming neutrons was 4.17 Å. The samples consisted of seven cylindrical plates of 12 mm diameter and 2.5 mm thickness. They were packed into a flat Al cassette. The scattering probability for thermal neutrons was less than 5%.

The measurements for the AlGe alloy were carried out at the five temperatures 4.9, 49, 122, 200 and 293 K. The measurements for $Al_{0.92}Si_{0.08}$ were carried out at 150 and 293 K and those for $Al_{0.88}Si_{0.12}$ at 100 and 293 K. The spectra from pure Al and the empty cryostat were also measured. The detector calibration was determined using a vanadium sample.

3.2. Data analysis

The measured spectra were corrected for background and detector efficiency and summed over all detectors. Figure 1 shows the room-temperature data for AlGe and AlSi alloys

together with the spectrum of pure Al. The behaviour of the high-energy part of the spectra of the AlGe and AlSi solid solutions is similar to that of pure Al. The most prominent difference is the strong peak around 9 meV in the AlGe alloy. This peak is not observed in the AlSi alloy, consistent with its interpretation as being due to a resonant mode of the heavy Ge atoms in the matrix of lighter Al atoms [11–14] similar to observations in the systems CuAu [15], CrW [16], TiU [17], AlAg [7] and others. The mass ratio between Ge and Al atoms is 2.7, while that between Si and Al atoms is only 1.03. Thus one expects resonant modes in the first case and not in the second, in agreement with the result shown in figure 1. This interpretation is further supported by a theoretical estimate of the expected neutron intensity on the basis of a pure mass defect picture for the metastable alloy with a concentration of 13 at.% Ge. The calculation is based on a simple incoherent approximation scheme at constant momentum transfer and resolution and is presented in figure 2.

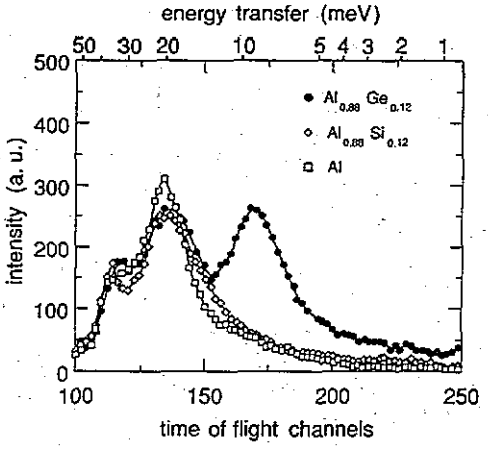

Figure 1. Room-temperature neutron time-of-flight data for pure Al and two non-equilibrium alloys with Si and Ge.

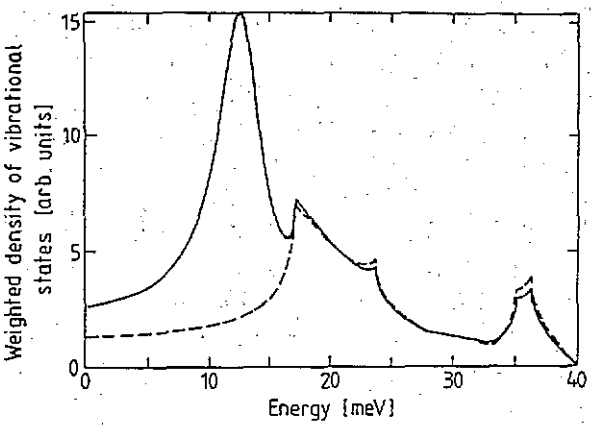

Figure 2. Calculated density of states for $Al_{0.87}Ge_{0.13}$ weighted with the scattering lengths and the frequency and temperature factors for inelastic neutron scattering at 120 K. The broken curve shows the pure Al signal for comparison.

The comparison of the AlSi and the pure Al spectra in figure 1 shows the broadening and the softening of the transverse zone boundary modes around 20 meV reported earlier [3]. Though overshadowed by the strong resonant mode peak, the same effect also exists in the AlGe case.

The temperature dependence of the inelastic scattering from the AlGe alloy is shown in figure 3. Data were measured at the four temperatures 49, 122, 200 and 293 K. The data points at 200 K were fitted by the smooth curve displayed in the figure. The other three full curves in figure 3 were obtained by scaling the 200 K curve with the appropriate Debye–Waller and Bose factor ratios to the three other temperatures. Though this scaling gives values that are too high at 293 K, it fits very well at the two lower temperatures over the whole measured frequency range. This holds in particular at the lowest frequencies. A crossover from harmonic to anharmonic behaviour with decreasing frequency as reported for vitreous silica [8] and amorphous polybutadiene [9] is not observed here. The deviations at room temperature do not invalidate this conclusion; on the one hand they have the opposite sign as compared to the glassy case [8, 9], and on the other hand we have to reckon with ageing effects at room temperature.

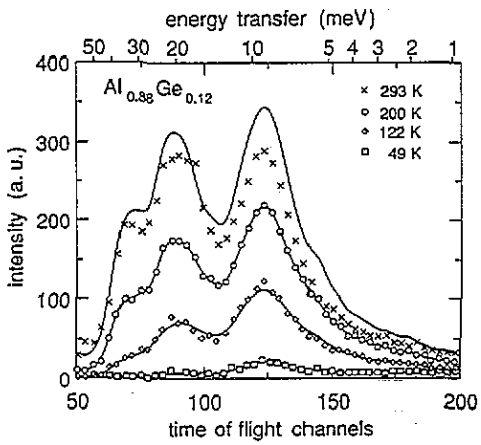

Figure 3. Temperature dependence of the time-of-flight spectrum of $Al_{0.88}Ge_{0.12}$. The full curves show the Debye–Waller and Bose scaling of the 200 K data as explained in the text.

The influence of this ageing was studied by measuring the inelastic neutron scattering spectra of the $Al_{0.88}Ge_{0.12}$ alloy at room temperature as a function of exposure time. Figure 4 shows spectra after 1 and 62 h at room temperature. The spectra are compared to that of pure Al and those of the alloy in the quenched metastable state at 122 K (corrected for temperature) and in the equilibrium state (obtained by annealing at 300 °C). The annealing decreases the resonant peak at 9 meV, probably due to gradual precipitation of Ge. For the equilibrium state this peak, slightly shifted to higher energy (about 10 meV) and lower in intensity, still exists and is explained as transverse zone boundary modes of precipitated crystalline Ge. As we will see in the following subsection, these ageing effects at room temperature also reduce the specific heat.

Figure 5 shows the dynamic structure factor for these vibrations in three different frequency windows. For the lowest frequency of 3.4 meV (figure 5(*c*)), one observes a relatively sharp peak centred around 2.7 $Å^{-1}$, the momentum transfer of the (111) reflection of the polycrystalline alloy. The sharpness of the peak allows us to conclude that these low-frequency vibrations of the non-equilibrium alloy are mainly long-wavelength modes with a wavelength around 40 Å as in pure Al at this frequency [18]. The dynamic structure factor for shorter wavelengths is markedly broader, as seen from the pure Al data in figure 5(*a*) and (*b*). We conclude that the excitations of the non-equilibrium alloys at 3.4 meV are essentially sound waves, again in contrast to the case of glasses [19]. Their density of states, however, seems to be a factor of 2–4 higher for $Al_{0.88}Si_{0.12}$ and a factor of 4–6

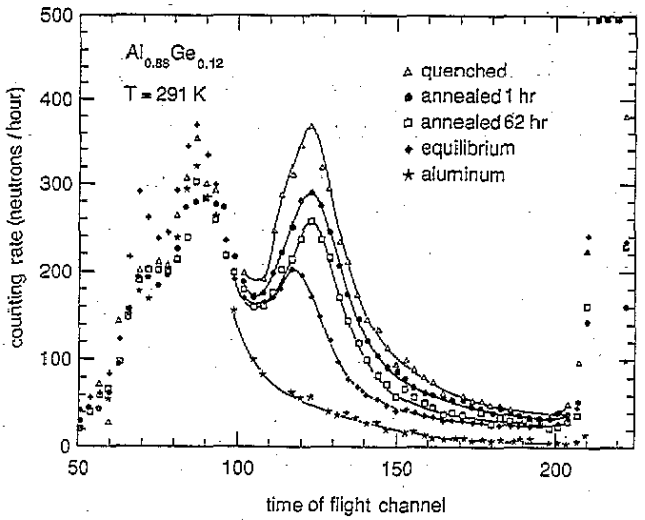

Figure 4. Effect of annealing at room temperature on the time-of-flight spectrum of $Al_{0.88}Ge_{0.12}$. Open triangles: quenched sample at 122 K, scaled up to room temperature; full circles: after annealing at 291 K for one hour; open squares: after 62 h; full diamonds: equilibrium state after annealing at 300 C; stars: pure Al.

higher for $Al_{0.88}Ge_{0.12}$ as compared to the density of states of pure Al. This finding is again corroborated by the specific heat results in the literature [4] and in the next subsection.

The resonant mode scattering from the heavy Ge atoms in the matrix of light Al atoms is clearly seen in figure 5(*b*). There the AlSi alloy and pure Al have comparable intensities, more than a factor of two lower than the intensity scattered from the AlGe alloy.

Our data are not as well suited for the determination of the generalized vibrational density of states as the data of Chevrier and co-workers [3] for two reasons. The first is an average over a relatively small range in momentum transfer (see figure 5). The second is the poor statistics of our cold-neutron measurement at high frequencies. This makes the normalization of the total density of states to unity a difficult task with questionable results. Nevertheless, we did such an evaluation, using the incoherent approximation and averaging over the experimental momentum transfer range. The results are shown in figure 6. They agree reasonably well with those given by Chevrier and co-workers [3], even in absolute numbers.

4. Specific heat

4.1. Experimental

The specific heat C_p was measured between 0.08 and 7.5 K in a dilution refrigerator using a transient heat pulse technique, with an arrangement very similar to that used earlier for $Al_{0.94}Si_{0.06}$ [4] and for amorphous superconductors [20]. In that technique, the sample is loosely linked to the regulated cold sink through the thermal resistance of a copper wire, which ensures the transient temperature decay after a heat pulse. The sample, in the present case in the form of a cylindrical platelet (1.90 g in weight), is clamped between two Si slices. The heater is fixed on one slice and the thermometer and the thermal link on the

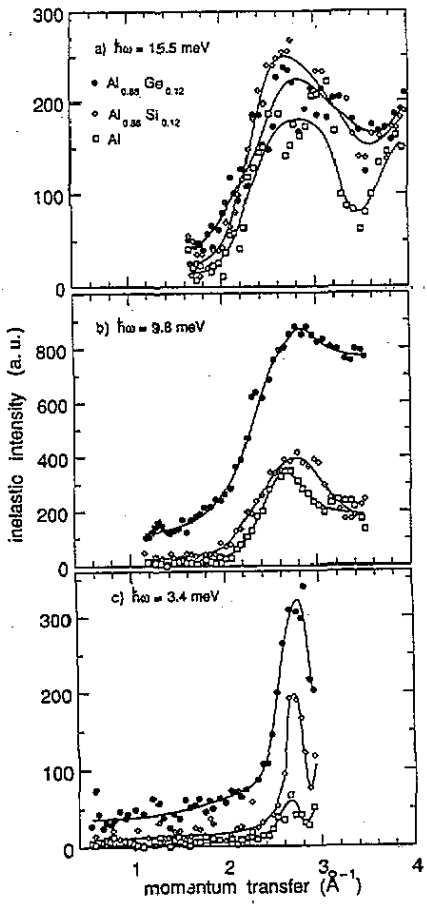

Figure 5. Dynamic structure factors for pure Al and two non-equilibrium alloys with Si and Ge at room temperature for three different frequencies: (a) 15.5 meV, (b) 9.8 meV and (c) 3.4 meV.

opposite slice. In almost the whole temperature range, the transients are well described by exponentials, except around and below 100 mK, where slight deviations from an exponential behaviour appear at long times, probably due to the presence of a nuclear contribution.

The sample, previously stored in liquid nitrogen, was held at room temperature for about four hours, the time necessary for its insertion into the sample holder and the transfer to the cryostat. The ageing effect during these four hours can be estimated from the decrease of the transition temperature to superconductivity T_c, as discussed below. After the first run, the sample was kept at room temperature for 9.5 d. Thereafter, for this 'aged' sample a second measurement was performed under practically identical conditions. In the following, we discuss first the results in the normal conducting state, then the jump of the specific heat at T_c and finally the low-temperature superconducting state.

4.2. Results and analysis

4.2.1. The normal state. In the normal state above T_c (see figure 7) C_p is, up to $T = 6.2$ K, well described by the usual $\gamma T + \beta T^3$ law, the sum of electronic and lattice contributions. One obtains $\gamma = 550\,\mathrm{erg\,g^{-1}K^{-2}}$ or $1.68\,\mathrm{mJ\,mol^{-1}\,K^{-2}}$ (molar mass = 30.63 g) and $\beta = 5.9 \times 10^{-5}\,\mathrm{J\,mol^{-1}\,K^{-4}}$ for the 'initial' state of the sample. The β parameter for the lattice contribution corresponds to a Debye temperature $\Theta_D = 320$ K. After ageing at 300 K, γ is slightly depressed by 1% to $1.67\,\mathrm{mJ\,mol^{-1}\,K^{-2}}$, whereas β remains unchanged. The main feature in figure 7 is a departure from linearity above $T^2 = 38\,\mathrm{K^2}$, which indicates

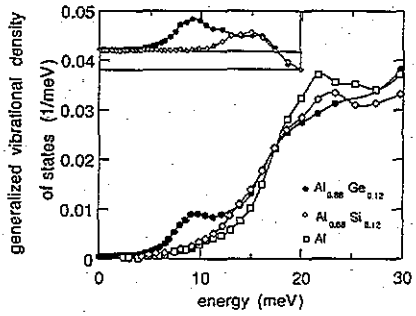

Figure 6. Evaluated density of states for pure Al and the two non-equilibrium alloys between 0 and 30 meV. The inset shows the deviations of the density of states of the two alloys from that of pure Al.

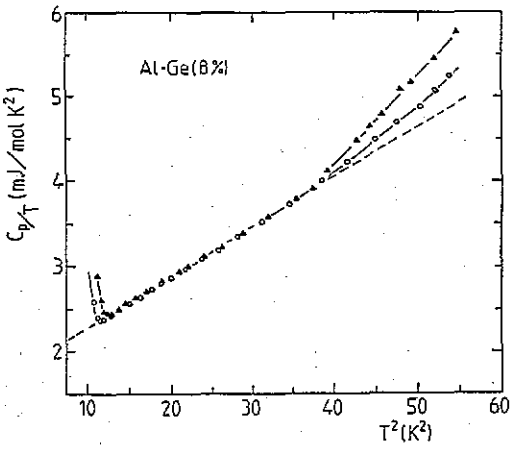

Figure 7. Specific heat C/T against T^2 above the transition to superconductivity (indicated by the upturn at the low-temperature end) for Al with 8 at.% Ge in the initial state (full triangles) and after ageing at 300 K (open circles). The broken curve shows the fit $\gamma T + \beta T^3$ for the initial state.

the presence of vibrational modes additional to the regular phonons. This deviation cannot be accounted for by an additional T^5 term in the lattice contribution, which would give a much slower departure from the T^3 law. It is ascribed to the resonant vibrational modes of the heavy-mass defect discussed above in the context of the neutron data. The ageing depresses this contribution, in qualitative agreement with the neutron results on ageing in figure 4.

4.2.2. The transition to superconductivity. The superconducting transition temperature T_c is defined by a jump of the electronic specific heat C_e. It is obtained from C_p by subtraction of the lattice term βT^3. We show in figure 8 C_e/T against T. The diagram enables the determination of T_c by the equalization of the entropy $\int (C_e/T)dT$ for both the experimental (extrapolated as shown in the broken curve) and an idealized jump at $T = T_c$. This method yields T_c =3.25 and 3.12 K for the initial and the aged states of the sample, respectively.

The measured values of the reduced jump parameter $\Delta C/\gamma T_c = 1.40$ to 1.44 for both samples agree within their accuracy with the BCS value of 1.43 for weak-coupling superconductors.

For $T_c/T \geqslant 1.5$, the electronic specific heat C_{es} of the superconductor decreases as $C_{es}/\gamma T_c = ae^{-bT_c/T}$. Our values ($a = 7.7$ to 7.8, $b = 1.4$) agree very well with those of the BCS theory (theoretical values $a = 8.5$, $b = 1.44$ for $1.5 \leqslant T_c/T \leqslant 7$). Note that for b the agreement is even better than the one found [21] for pure Al ($b = 1.34$). The deviation in the pure case has been ascribed to energy gap anisotropy. Such an effect can be removed by the introduction of impurities, acting as scattering centres which let C_{es} be determined by a single average gap and results in a behaviour closer to the BCS one [22]. This is probably the case for Al doped with Ge or Si. In addition, we have verified the consistency of the electronic contribution between normal and superconducting states by comparing the entropies of both states. For the electronic coefficient γ_s, determined below T_c via

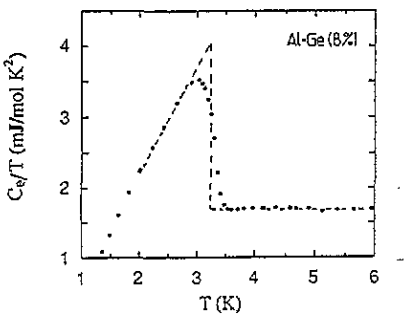

Figure 8. Electronic specific heat jump at T_c for the initial state, plotted as C_e/T against T. The broken curves indicate the idealized jump as explained in the text. In particular, the horizontal line above T_c represents γ.

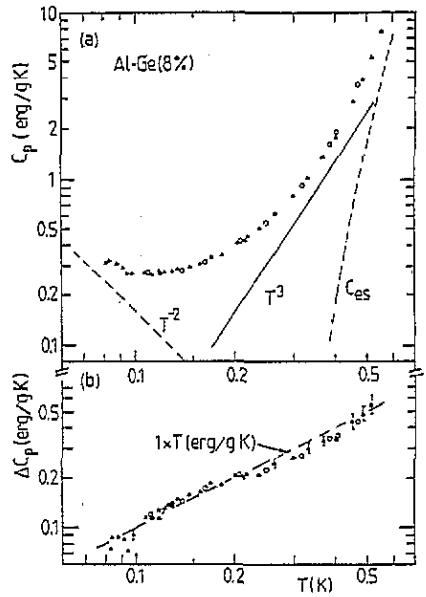

Figure 9. (*a*) Total specific heat below 0.6 K in a log–log plot, for Al with 8% Ge in the initial state (full triangles) and after ageing at 300 K (open circles). C_{es} represents the electronic superconducting contribution, exponentially decreasing; T^3, the lattice term; T^{-2} is the hyperfine nuclear contribution (0.0016 erg K g^{-1}). (*b*) Residual contribution, having subtracted the C_{es}, T^3 and T^{-2} contributions from the total C_p, both for the initial state (full triangles) and after ageing at 300 K (open circles).

$$\int_0^{T_c} C_{es}/T\,dT = \int_0^{T_c} C_{en}/T\,dt = \gamma_s T_c \tag{1}$$

we find values which agree within 2% with the γ value defined above T_c for both the initial and the aged sample. Note that this analysis is done using the same lattice T^3 term in the superconducting and in the normal state.

4.2.3. The range well below T_c. Below 0.6 K, the data analysis indicates a small additional contribution, as seen in figure 9(*a*) by the progressive deviation from a T^3 law at low temperatures. The slight upturn of C_p below 0.1 K is probably due to a small nuclear hyperfine contribution $C_N T^{-2}$, either intrinsic, due to Ge atoms (electric quadrupolar), or extrinsic, due to magnetic impurities. Moreover, there seems to be a small linear term, reminiscent of the one found in glasses [23]. We can describe the specific heat in this temperature region as a sum of four terms

$$C_p = C_{es} + \beta T^3 + C_N T^{-2} + aT \tag{2}$$

where $a = (1 \pm 0.1)$ erg g^{-1} K^{-2} between 0.08–0.5 K. This term remains unchanged in the aged state (figure 9(*b*)).

5. Discussion

5.1. Frequency ranges of neutron and specific heat data

Let us begin the discussion by considering the frequency ranges of the inelastic neutron scattering data on the one hand and the specific heat data on the other. The frequency range of our neutron experiment is limited at low frequencies by the resolution of 0.2 meV. At high frequencies, one sees in principle the entire spectrum, but the necessity to work in the energy gain of the neutrons together with the low energy (4.7 meV) of the incoming neutrons limits the range of evaluation effectively to about 25 meV. Thus the frequency range of the neutron data spans practically the whole region of sound waves including the transverse zone boundary modes.

The specific heat at low temperatures is essentially due to excitations with frequencies of the order of $4k_BT/h$ (where k_B is the Boltzmann constant and h is the Planck constant). The measured temperature range from 80 mK to 7.5 K translates into a frequency range from 30 μeV to 3 meV, overlapping and extending the range of the neutron study to lower frequencies.

In the following, we discuss the findings of both methods in the order of decreasing frequency of the excitations, beginning with the transverse zone boundary at 25 meV and the resonant Ge modes at 9 meV.

5.2. Zone boundary and resonant heavy-atom modes

For the zone boundary modes, the analysis of the neutron data (see figure 6) corroborates the metallic-glass-like softening reported earlier by Chevrier and co-workers [3]. This finding had encouraged the hope to be able to study glass-like anomalies in a simple crystalline system. In fact, the AlGe system [6] seemed to show a further glass-like anomaly [24], namely a peak in the scattering at 9 meV, well below the transverse zone boundary peak. However, since the 9 meV peak is absent in the AlSi case, it has to be assigned to the resonant mode of a heavy Ge atom in the host lattice of light Al atoms. The low-frequency tail of these modes causes the upturn of the specific heat from the Debye T^3 behaviour at the high-temperature end of our measurement in figure 7. Note the absence of this upturn in AlSi [4], where no resonant modes exist.

5.3. The sound wave range from 0.5–5 meV

In the frequency range around 2 meV, both neutron and specific heat data show a density of states of the alloys which is about a factor of three higher than the one of pure Al. This enhancement, however, does not seem to be due to additional localized vibrational modes coexisting with the sound waves (our present picture for glasses [25]), but rather to a lowering of the sound velocities. In the neutron case, this is indicated by the dynamic structure factor in figure 5(*c*), which is as sharply centred around the Bragg position as in pure Al. It is further evidenced by the absence of anharmonic effects in the temperature dependence of the neutron signals at low frequencies, in contrast to vitreous silica [8] or amorphous polybutadiene [9] (compare figure 3). In the specific heat, the sound wave character is seen from the large range of validity of the T^3 law in figure 7, again in contrast to the much steeper rise of the specific heat of typical glasses at these temperatures [25]. Naturally, the existence of glass-like modes cannot be excluded completely, but clearly they seem to be less abundant in these alloys than in glasses.

5.4. Electronic properties and the transition to superconductivity

As in the AlSi quenched metastable solid solutions, compared to pure Al, one observes in the specific heat data an increase of the linear electronic term γ and a decrease in the Debye temperature Θ_D. For pure Al [21], $\gamma = 1.35\,\mathrm{mJ\,mol^{-1}\,K^{-2}}$ and $\Theta_D = 428\,\mathrm{K}$. Both properties, the increase of the electronic density of states at the Fermi energy and the decrease of the Debye temperature, result in an increase of the electron–phonon coupling and hence of T_c. Using the McMillan equation [26]

$$\lambda = \frac{\mu^* \ln(\Theta_D/1.45T_c) + 1.04}{(1 - 0.62\mu^*)\ln(\Theta_D/1.45T_c) - 1.04} \tag{3}$$

where $\mu^* = 0.1$ (usually assumed for the effective Coulomb potential), we can estimate the electron–phonon interaction constant λ to be about 0.5 ($\lambda = 0.38$ for Al and 0.48 for AlSi [4]). The decrease of the Debye temperature to 320 K in our AlGe alloy is larger than in AlSi of similar composition ($\Theta_D = 384$ and about 375 K for 6 and 8 at.% Si, respectively).

A second property which is similar to the AlSi system is the excellent agreement of the superconducting thermodynamical behaviour with the BCS theory for weak electron–phonon coupling. In particular, one recovers the full specific heat jump and a total electronic condensation for C_{es} below T_c. This indicates that the whole sample is involved in the transition. We note that there is no modification of the lattice term in the superconducting state.

5.5. Low-temperature linear term in the specific heat

Well below the superconducting transition temperature, there seems to be a linear contribution to the specific heat reminiscent of the contribution of two-level states in amorphous materials [23]. It is smaller than the one found in the AlSi system ($a = 1\,\mathrm{erg\,g^{-1}\,K^{-2}}$ in our case compared to $3.4\,\mathrm{erg\,g^{-1}\,K^{-2}}$ in Al with 6% Si and values between 6–10 in typical amorphous metallic alloys). If we interpret this term as being due to two-level states, we obtain a density of states $n_0 = 6a/(\pi^2 k_B^2) \approx 10^{45}$ states per Joule and m^3.

The linear term could in principle be due to small amorphous clusters of segregated Ge resulting from the initial annealing. However, such a hypothesis does not seem probable. Firstly, small-angle neutron scattering [27] shows a precipitation of Ge into small balls with about 80 Å diameter. In the first fifteen hours at room temperature, the number of these balls increased with time, while their diameter did not change markedly. Afterwards, the precipitation slowed down. The wide-angle scattering showed Bragg-like peaks with full widths at half maximum ΔQ of $0.25\,\mathrm{Å^{-1}}$ after five hours and $0.15\,\mathrm{Å^{-1}}$ after 43 h. The latter value is consistent with a crystalline cluster size of 80 Å. The data show that the aged state of the sample consists of crystalline semiconductor clusters in a matrix of an AlGe solid solution. Secondly, the linear specific heat term of amorphous Ge is unusually small [28], namely $a \leqslant 2\,\mathrm{erg\,g^{-1}\,K^{-2}}$. Even if the whole Ge content were present as amorphous Ge, the linear term would still be a factor of five lower than the observed one. In addition, there is no evolution of the linear term with ageing. We conclude that the main part of the linear term is, as in the AlSi system, intrinsic in the metastable solid solution.

5.6. Role of ageing at 300 K

The superconducting transition temperature T_c in the 'as-quenched' state (3.5 ± 0.1 K) decreases by 0.25 K after ageing for about four hours at room temperature and by a further decrease of 0.12 K after 9.5 more days. The only other significant variation concerns the contribution of the heavy-defect modes. This seems to be very sensitive to ageing. It decreased by more than a factor of two by the second annealing at room temperature. The lattice term and the linear terms remained unaffected.

6. Conclusions

Though the non-equilibrium pressure-quenched solutions of Si and Ge in Al show a softening of the transverse zone boundary modes similar to the one observed in metallic glasses, they do not seem to be good candidates for the study of glassy anomalies in a simple crystalline system. Additional vibrations at 9 meV in AlGe are absent in AlSi and can be explained semiquantitatively in terms of resonant modes of a heavier atom in a host lattice of lighter atoms. Between 0.5 and 5 meV, a region where in glasses localized soft vibrations outnumber the sound waves [25], one finds only sound waves in these alloys within the experimental accuracy. The conclusion is partly corroborated by the linear term in the specific heat at very low temperatures, which is much smaller than in typical glasses.

The electronic contribution to the specific heat follows the classical BCS behaviour below T_c, indicating that the whole sample is involved in the superconducting transition.

Acknowledgments

One of us (AIK) wants to acknowledge the support of the Alexander von Humboldt foundation during his stay in Germany.

References

[1] Degtyareva V F, Chipenko G V, Belash I T, Barkalov O I and Ponyatovskii E G 1985 *Phys. Status Solidi* a **89** K127
[2] Degtyareva V F, Chipenko G V, Ponyatovskii E G and Rashchupkin V I 1984 *Sov. Phys.–Solid State* **26** 733
[3] Chevrier J, Suck J B, Capponi J J and Perroux M 1988 *Phys. Rev. Lett.* **61** 554
[4] Chevrier J, Lasjaunias J C, Zougmore F and Capponi J J 1989 *Europhys. Lett.* **8** 173
[5] VanCleve J E, Chevrier J and Pohl R O 1990 *Phonons 89* ed S Hunklinger, W Ludwig and G Weiss (Singapore: World Scientific) p 579
[6] Kolesnikov A I, Prager M, Schober H R, Buchenau U, Barkalov O I, Belash I T and Ponyatovskii E G 1989 *Dynamics of Disordered Materials (Springer Proceedings in Physics 37)* ed D Richter, A J Dianoux, W Petry and J Teixeira (Berlin: Springer) p 191
[7] Zinken A, Buchenau U, Fenzl H J and Schober H R 1977 *Solid State Commun.* **22** 693
[8] Buchenau U, Zhou H M, Nücker N, Gilroy K S and Phillips W A 1988 *Phys. Rev. Lett.* **60** 1318
[9] Frick B and Richter D 1989 *Dynamics of Disordered Materials (Springer Proceedings in Physics 37)* ed D Richter, A J Dianoux, W Petry and J Teixeira (Berlin: Springer) p 38
[10] Hansen M and Anderko K 1958 *Constitution of Binary Alloys* (New York: McGraw-Hill)
[11] Krivoglaz M A 1961 *Zh. Eksp. Teor. Fiz.* **40** 567 (Engl. transl. 1961 *Sov. Phys.–JETP* **13** 397)
[12] Kagan Yu and Iosilevskii Ya 1963 *Zh. Eksp. Teor. Fiz.* **44** 1375 (Engl. transl. 1963 *Sov. Phys.–JETP* **17** 925)
[13] Brout R and Visscher W M 1962 *Phys. Rev. Lett.* **9** 54
[14] Elliott R J and Brockhouse B N 1965 *Inelastic Scattering of Neutrons* (Vienna: IAEA)

[15] Svensson E C, Brockhouse B N and Rowe J M 1965 *Solid State Commun.* **3** 245
[16] Moeller B H and Mackintosh A R 1965 *Phys. Rev. Lett.* **15** 623
[17] Chernoplekov N A, Panova G Kh, Zemlyanov M G, Samoilov B N and Kutaitsev V I 1967 *Phys. Status Solidi* **20** 767
[18] Buchenau U 1979 *Solid State Commun.* **32** 1329
[19] Buchenau U, Prager M, Nücker N, Dianoux A J, Ahmad N and Phillips W A 1986 *Phys. Rev.* B **34** 5665
[20] Zougmore F, Lasjaunias J C and Bethoux O 1989 *J. Physique* **50** 1241
[21] Phillips N E 1959 *Phys. Rev.* **114** 676
[22] Phillips N E 1971 *Critical Reviews in Solid State Science* (Boca Raton, FL: Chemical Rubber Company) p 500
[23] Phillips W A 1972 *J. Low Temp. Physics* **7** 351
Anderson P W, Halperin B I and Varma C M 1972 *Phil. Mag.* **25** 1
[24] Malinovsky V K, Novikov V N, Parshin P P, Sokolov A P and Zemlyanov M G 1990 *Europhys. Lett.* **11** 43
[25] Buchenau U, Galperin Yu M, Gurevich V L and Schober H R 1991 *Phys. Rev.* B **43** 5039
[26] McMillan W L 1981 *Phys. Rev.* **79** 161
[27] Kolesnikov A I, Ostanevich Yu M, Barkalov O I and Ponyatovsky E G (unpublished)
[28] Löhneysen H L and Schink H J 1982 *Phys. Rev. Lett.* **48** 1121